Optoelectronic properties of transparent and conducting single-wall carbon nanotube thin films

Giovanni Fanchini,[a] Husnu Emrah Unalan, and Manish Chhowalla
Materials Science and Engineering, Rutgers University, Piscataway, New Jersey 08854

(Received 14 December 2005; accepted 12 April 2006; published online 12 May 2006)

Optoelectronic characterization of transparent and conducting single-wall carbon nanotube thin films is reported. By eliminating the influence of voids and bundle-bundle interactions within the effective medium theory, we show that the complex dielectric response of the individual nanotube varies with its density in the film. Specifically, the absorption peak assigned to the maximum intensity of π-π^* transitions was found to decrease from E_π=5.0 eV at low nanotube density to E_π=4.2 eV at intermediate densities and increased again at higher densities to E_π=4.5 eV. Furthermore, the Drude background was found only above a critical density (Φ_o) of nanotubes. These results unequivocally demonstrate that the optical processes are not confined only to in-tube transitions and that the absence of confinement in nanotube networks profoundly affects the electronic behavior of the individual tube. © *2006 American Institute of Physics*.
[DOI: 10.1063/1.2202703]

Single-wall carbon nanotubes (SWNTs) exhibit remarkable electronic[1] and optical[2] properties. Transparent and conducting SWNT thin films[3] are low density networks that take advantage of the excellent electronic properties of SWNTs.[3,4] Their transparency[5,6] can be higher than 90% and they can be prepared at room temperature by transferring onto the desired substrates using a variety of techniques.[3,4] Thus far, optoelectronic characterization of transparent and conducting SWNT thin films has been performed[2] using models developed for directly grown carbon nanotubes which are denser and possess little transparency. Interesting features such as the role of the percolation threshold in determining the electrical properties of SWNT thin films have only recently been explored.[5,6] In the previous reports,[5,6] the optical properties have been studied mainly at normal incidence and interpreted using the standard model for metallic thin films. The model[5] assumes that the ratio between the static (direct current) conductivity and the optical conductivity remains constant at any given photon energy. If valid, this assumption has far reaching consequences. It implies that the dielectric function of the SWNT thin films is determined by the concentration of the SWNTs only, while the dielectric response of the individual nanotube would be the same in isolated SWNTs, where electron confinement effects are expected to dominate, and in SWNT thin films, where the confinement is released due to variable connectivity in the network. However, it is not immediate that the dielectric response of the individual SWNT is the same in confined and nonconfined systems.

In this letter, we elucidate the effects of confinement in transparent and conducting SWNT thin films by focusing on their in-plane optoelectronic properties obtained using spectroscopic ellipsometry at low grazing angles. We determine the optical response of the individual SWNT in networks at different densities, getting rid of effects of the environment within the effective medium theory. Our results suggest that confinement effects are not insignificant and cannot be ignored because they influence the photon energies (E_π) for the π-π^* transitions. On the other hand, the films exhibit metallic optical properties only above a critical density (Φ_o) of the network, even though metallic SWNTs are present below such a threshold since they represent one-third of the overall nanotubes.[1]

SWNTs (HiPCO) were purchased from Carbon Nanotechnologies, Inc. and thoroughly purified by reiterative low temperature oxidative annealing and acid treatment. The purified SWNTs were then sonicated for 2 h in 1 wt % sodiumdodecyl-sulfate water solutions in order to obtain a uniform and stable suspension. The SWNT thin films were deposited using the method of Wu *et al.*[4] Briefly, a 200 nm pore size nitrocellulose filter membrane was used to filter a controlled volume of SWNT suspension. The filter was then transferred onto optical grade fused silica substrates and dissolved in acetone and methanol, leaving behind uniform SWNT thin films. The SWNT concentration in the suspension was kept constant at 2 mg/l for the samples reported in this study.

A range of SWNT thin films at varying filtration volumes (V_{sol}=10–70 ml) were deposited. The variation in density of SWNTs in the thin film network as a function of the filtered suspension volume can be seen from the SEM images in Fig. 1. Three different morphologies can be observed with increasing filtrated volume. Initially [Fig. 1(a)], a semicontinuous network with a dominant fraction of void space can be seen. Increasing the filtration volume [Fig. 1(b)] leads to a SWNT network with still visible voids. Further increase in the filtrated volume leads to a continuous network [Fig. 1(c)].

Our transparent and conducting SWNT films were investigated using a Jobin-Yvon UVISEL spectral ellipsometer. The ellipsometric angles Δ_m and Ψ_m measured at an incidence angle of 70°, are plotted in Figs. 2(a–b). We observed strong differences in the spectra for films deposited above and below the critical filtrated volume of 50 ml. In order to investigate the mechanism responsible for this variation, the inversion of the ellipsometric equations was performed using the numerical iterative procedure described by Azzam and Bashara,[7]

[a]Author to whom correspondence should be addressed; electronic mail: fanchini@rci.rutgers.edu

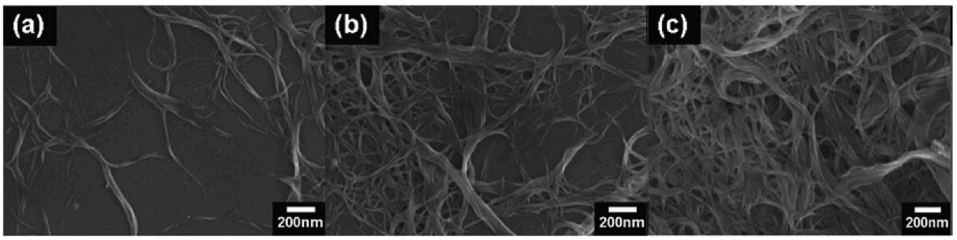

FIG. 1. SEM images of SWNT films with a filtrated volumes of (a) 20 ml, (b) 40 ml, and (c) 60 ml. The SWNT concentration in the suspension was kept constant at 2 mg/l for all the samples. The electron microscopy studies were performed on a LEO Zeiss Gemini 982 field emission scanning electron microscope (SEM) operated at 5 kV.

$$\Psi_m - \Psi(\varepsilon,\Phi) = 0 \quad \Delta_m - \Delta(\varepsilon,\Phi) = 0. \tag{1}$$

As a starting point for our numerical refinement, we assumed the thin films to be formed by a fraction (Φ) of a semi-infinite SWNT medium [complex dielectric response $\varepsilon_{NT}(E)=\varepsilon_{1NT}(E)+i\varepsilon_{2NT}(E)$] and a fraction $(1-\Phi)$ of voids (dielectric constant $\varepsilon_0 \approx 1$), as shown in Fig. 2(c). The dielectric function $\varepsilon' = \varepsilon_1'(E) + i\varepsilon_2'(E)$ for such a case can be analytically obtained.[7] Subsequently, the real $[\varepsilon_1(E)]$ and imaginary $[\varepsilon_2(E)]$ parts of the complex dielectric function were iteratively refined by modeling within the Bruggeman effective medium theory (EMT)[8] as in Fig. 2(d). A generalized EMT for nonspherically shaped particles and voids derived by Cohen *et al.*[9] was used,

$$\frac{\Phi(\varepsilon_{NT}-\varepsilon)}{q\varepsilon_{NT}+(1-q)\varepsilon} + \frac{(1-\Phi)(\varepsilon_0-\varepsilon)}{q_0\cdot\varepsilon_0+(1-q_0)\varepsilon} = 0, \tag{2}$$

and the dielectric function $[\varepsilon(E)]$ of the effective medium was extracted. $\Psi[\varepsilon(E)]$ and $\Delta[\varepsilon(E)]$ were then recalculated and the relative mean square difference with the measured quantities, $\Psi_m(E)$ and $\Delta_m(E)$, was iteratively minimized via Eq. (1). In Eq. (2), the depolarization factors q and q_0 account for the peculiar geometry of the particles and the host medium, respectively. Depolarization factors take values of $q=\frac{1}{3}$ for interacting particles with spherical symmetry, $q=\frac{1}{2}$ for interacting disks and tubes, and $q=q_0=0$ for noninteracting particles.[9] The q factors for our samples are reported in Fig. 3(a). It can be observed that q increases with the filtrated volume, consistent with decreasing intertube distance while at higher density it tends to $\frac{1}{2}$.

Figures 3(b–c) show the dielectric responses of the SWNTs in our films after the effects of the voids and bundle-bundle interactions have been eliminated by means of Eqs. (1)–(2). Below the critical volume of 50 ml, $\varepsilon_{2NT}(E)$ typically exhibit a broad peak shifting from $E_\pi=5.0$ eV (at 10 ml) to $E_\pi=4.25$ eV (at 40 ml), as shown in Fig. 3(b). Such a downshift suggests that ε_{NT} depends on the amount of confinement. The maximum intensities of the π-π^* transitions in individual SWNTs [$E_\pi=5.74$ eV (Ref. 1)] is indeed higher. In graphite the maximum intensity of the π-π^* interband transitions occur at 4.5 eV and it is superimposed on the metallic Drude background.[10] It is therefore interesting to notice that, once reaching a minimum at $V_{sol}=40$ ml, E_π increases again in more connected SWNT networks [$V_{sol}=50-70$ ml, Fig. 3(c)], approaching the value in graphite. Several reasons such as strong SWNT-SWNT interactions which cannot be described at a dipole-dipole level,[8,9] the reduction of the π-bond strength due to disorder, different levels of anisotropy in different samples, or excitonic effects[11] could lead to the observed trend of E_π. In any case, our results clearly show that the dielectric response of the nanotubes is sample dependent and the reduction in electronic confinement plays a non-negligible role.

In addition to the different π-π^* peak values, other important changes in the electronic structure of the films occur at approximately 50 ml, as can be observed by comparing Figs. 3(b) and 3(c). The immediately noticeable difference is that $\varepsilon_{2,NT}(E)$ clearly diverges at low photon energies only above 40 ml, making the optical spectra similar to those of graphite.[10] Such a low-energy divergence of $\varepsilon_2(E)$ is increasingly important at 50–70 ml where it can be fitted in the framework of the Drude model for metals which is a definite indication of metallic conductivity.[10] The Drude background is absent below 50 ml. Thus, the presence of metallic SWNTs is not a sufficient condition for metallic conductivity as long as bundles are not interconnected to each other. The metallic behavior in a network arises when the network is percolating. We can therefore conclude that at 2 mg/l concentration of SWNTs, the optical metallic percolation threshold is about 40–50 ml.

In contrast, the percolation threshold estimated by electrical measurements is lower than that obtained by ellipsometry. In systems of sticks close to the percolation threshold Φ_c, the metallic conductivity follows the expression:[5,12]

$$\sigma = \sigma_{met}(\Phi - \Phi_c)^n, \tag{3}$$

where σ_{met} depends on the conductance of the single metallic SWNT. In the framework of a two-dimensional model of our sample, Φ should depend only on the

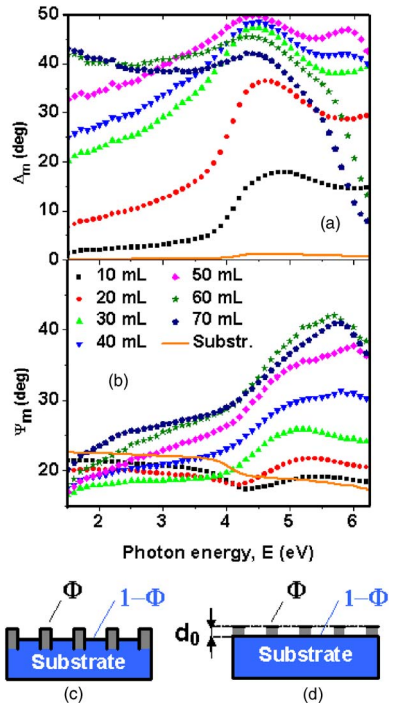

FIG. 2. (Color online) Ellipsometric angles: (a) Δ_m, (b) Ψ_m, (c) Starting analytic model assuming a fraction Φ of SWNTs as a semi-infinite medium not interacting with the host medium. (d) Numeric model assuming semi-transparent bundles interacting at a dipole-dipole level (EMT).

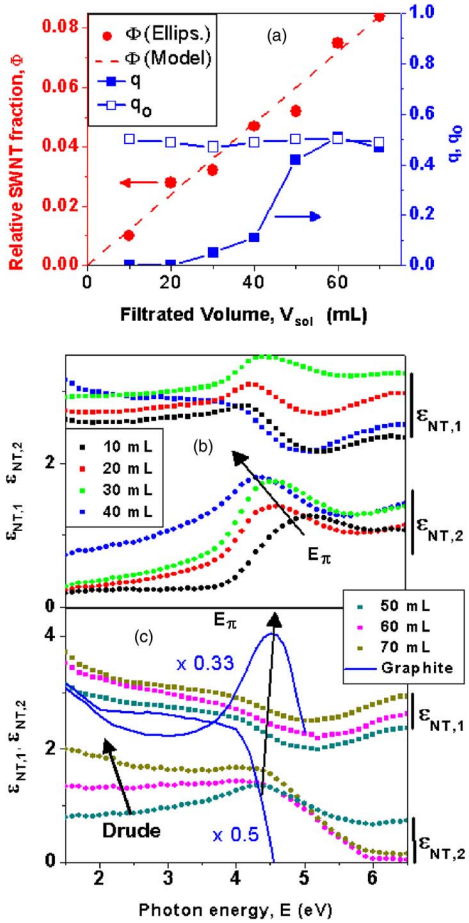

FIG. 3. (Color online) (a) Modeling parameters used to determine the dielectric response of the individual tube. (b-c) Calculated dielectric functions $\varepsilon_{1NT}(E)$ and $\varepsilon_{2NT}(E)$ of the single tube, as a function of the photon energy E. Remarkable effects of confinement are the shifts of E_π, and the appearance of the Drude background at 50 ml, indicating the onset of metallic optical behavior.

filtrated volume of the solution (V_{sol}), its concentration (x_{sol}), the area A_0 of the filter, and the density of SWNTs [i.e., $\rho_{NT}=1.3$ g cm^{-3}, which is the average nominal density of SWNTs with diameters of 1–2 nm at different chiralities (Ref. 1)]. The average film thickness can be estimated to be $d_0 \approx L\cdot\langle\sin\theta\rangle$, depending on the tube length ($L\approx 1$ μm) and their random orientation θ. Under such assumptions, a straightforward calculation[6] leads to $\Phi=(x_{sol}V_{sol}/\rho_{NT})/(A_0 d_0)\approx 6\times 10^{-4}\cdot x_{sol}(\text{mg/l})\cdot V_{sol}(\text{ml})$. The ellipsometry data agree well with Φ calculated using this relationship, corresponding to the dotted line in Fig. 3(a).

A fit of the conductivities of our films in terms of Eq. (3) is presented in Fig. 4 (inset) and gives $\Phi_c=0.0055$, a value much lower than $\Phi_o=0.05$ ($V_{sol}=50$ ml) corresponding to the appearance of the Drude background. The data in Fig. 4 show that only at solution concentrations of $x_{sol}<2$ mg/l, nonpercolating behavior in the transport properties is observed, as indicated by the departure from Eq. (3) at $\Phi<\Phi_c$ and the resulting exponential behavior of conductivity. Thus, we argue that the percolation thresholds obtained

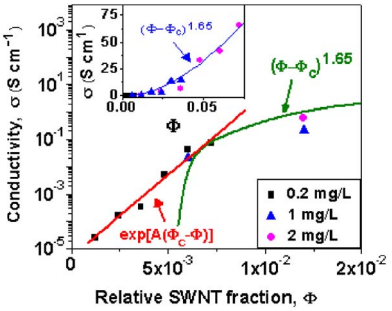

FIG. 4. (Color online) Direct current electrical conductivity vs SWNT fraction in transparent conducting SWNT thin films. Data from Ref. 6, ($x_{sol}=0.2$ mg/l and $x_{sol}=1$ mg/l) are added, since all the samples considered in the present study ($x_{sol}=2$ mg/l) are electrically percolating.

by electrical (Φ_c) and optical (Φ_o) measurements differ.

In summary, we report two remarkable observations on the optoelectronic behavior of transparent and conducting SWNT thin films. Firstly, we derived the dielectric response of the individual SWNT, separating it from the dielectric function of the host medium. Getting rid of the effects of the voids and the bundle-bundle interactions in the framework of the EMT, we show that the dielectric function of the individual SWNT varies from sample to sample depending on the intertube distance and hence on the electronic confinement. Secondly, we show that a percolation threshold can be extracted from the analysis of the optical properties but it is somewhat higher than what is obtained from the electrical data.

The authors would like to thank the RU-Academic Excellence Fund for financial support and Prof. D. Birnie for the use of the ellipsometer.

[1] *Carbon Nanotubes Synthesis, Structure, Properties and Applications*, edited by M. S. Dresselhaus, G. Dresselhaus, and P. Avouris (Springer, New York 2001).
[2] W. D. Heer, W. S. Bacsa, A. Chatelain, T. Gerfin, R. H. Baker, and L. Forro, Science **268**, 845 (1995).
[3] M. D. Lay, J. P. Novak, and E. S. Snow, Nano Lett. **4**, 603 (2004); N. Saran, K. Parikh, D. S. Suh, E. Munoz, H. Kolla, and S. K. Manohar, J. Am. Chem. Soc. **126**, 4462 (2004); M. A. Meitl, Y. Zhou, A. Gaur, S. Jeon, M. Usrey, M. S. Strano, and J. A. Rogers, Nano Lett. **4**, 1643 (2004); E. Artukovic, M. Kaempgen, D. S. Hecht, S. Roth, and G. Gruner, *ibid.* **5**, 757 (2005).
[4] Z. Wu, Z. Chen, X. Du, J. M. Logan, J. Sippel, M. Nikolou, K. Kamaras, J. R. Reynolds, D. B. Tanner, A. F. Hebard, and A. G. Rinzler, Science **305**, 1273 (2004).
[5] L. Hu, D. S. Hecht, and G. Gruner, Nano Lett. **4**, 2513 (2004).
[6] H. E. Unalan, G. Fanchini, A. Kanwal, A. Du Pasquier, and M. Chhowalla, Nano Lett. **6**, 667 (2006).
[7] R. M. A. Azzam and N. M. Bashara, *Ellipsometry and Polarized Light* (North-Holland, Amsterdam, 1987).
[8] D. A. G. Bruggeman, Ann. Phys. **24**, 636 (1935).
[9] R. W. Cohen, G. D. Cody, M. D. Cutts, and B. Abeles, Phys. Rev. B **8**, 3689 (1973).
[10] *Handbook of Optical Constant of Solids*, edited by E.A. Palik (Academic, New York, 1975), Vol. 1.
[11] F. Wang, G. Dukovic, L. E. Brus, and T. F. Heinz, Science **308**, 838 (2005).
[12] D. Stauffer and A. Aharony, *Introduction to Percolation Theory* (Taylor & Francis, London, 1992).